fMRI Biomarker of Early Neuronal Dysfunction in Presymptomatic Huntington's Disease

Jane S. Paulsen, Janice L. Zimbelman, Sean C. Hinton, Douglas R. Langbehn, Catherine L. Leveroni, Michelle L. Benjamin, Norman C. Reynolds, and Stephen M. Rao

BACKGROUND AND PURPOSE: Functional MR imaging (fMRI) has been used to probe basal ganglia function in people with presymptomatic Huntington's disease (pre-HD). A previous fMRI study in healthy individuals demonstrated activation of the basal ganglia during a time-discrimination task. The current study was designed to examine the relative sensitivity of fMRI compared with that of behavioral testing and morphometric measurements in detecting early neurodegenerative changes related to Huntington's disease (HD).

METHODS: Pre-HD participants were assigned to two groups based on estimated years to diagnosis of manifest disease: close <12 years and far ≥12 years. Age at disease onset was estimated using a regression equation based on the number of trinucleotide CAG repeats. The time-discrimination task required participants to determine whether a specified interval was shorter or longer than a standard interval of 1200 milliseconds.

RESULTS: Participants in the close group performed more poorly on the time-task discrimination than did control subjects; however, no differences were observed between far participants and control subjects. Similarly, close participants had reduced bilateral caudate volume relative to that of control subjects, whereas far participants did not. On functional imaging, close participants had significantly less activation in subcortical regions (caudate, thalamus) than control subjects; far participants had an intermediate degree of activation. In contrast, far participants had hyperactivation in medial hemispheric structures (anterior cingulate, presupplementary motor area) relative to close and control subjects.

CONCLUSION: Hyperactivation of medial prefrontal regions compensated for reduced subcortical participation during time discrimination in pre-HD. This pattern of brain activation may represent an early neurobiologic marker of neuronal dysfunction.

Huntington's disease (HD) is an autosomal-dominant, neurodegenerative disorder that results from an expansion of the trinucleotide repeat CAG in gene IT-15 that encodes the protein called huntingtin on chromosome 4 (1). The disease is principally characterized by degeneration in the caudate and putamen (2, 3), although reports suggest neuron loss in cortical layers 3, 5, and 6 as well (4–6). Clinical features typically emerge in middle adulthood and include movement disorder, cognitive deterioration, and psychiatric symptoms. The diagnosis is made at the emergence of motor symptoms, although structural and metabolic brain changes, neuropsychological deficits, and psychiatric symptoms often precede the manifestation of neurologic disease in presymptomatic individuals who have the HD mutation (7–10).

There is currently no treatment or cure for HD; however, compounds have been developed that slow symptom progression in animal models, prompting a series of human clinical trials currently underway (11, 12). Ideally, potential treatments should target at-risk individuals at the earliest stage of neural degeneration, before functional decline occurs. The development of prevention guidelines, however, depends on the ability to predict future disease onset and to detect subtle pathologic changes before consequences manifest. The current study was performed to determine whether functional MR imaging (fMRI) can detect early signs of neural abnormality in pre-HD individuals.

Subject demographics, CAG repeat size, and test scores

	Participants		
Measure	Far	Close	Control
Age (years)*	33.0 (5.0)	41.1 (5.9)	38.0 (6.1)
Education (years)	14.6 (2.4)	14.1 (1.7)	14.9 (1.9)
Sex (M/F)	(2/5)	(4/3)	(2/5)
CAG repeat size†	41.3 (2.1)	44.2 (2.5)	NA
Estimated years to symptom onset‡	24.6 (7.9)	8.6 (2.5)	NA
UHDRS motor score	0.7 (1.0)	1.4 (0.9)	NA
UHDRS verbal fluency	39.9 (11.7)	32.9 (8.7)	39.4 (6.4)
UHDRS symbol-digit	57.3 (10.0)	44.9 (8.8)	52.4 (10.9)
UHDRS stroop interference	50.9 (13.1)	37.1 (12.2)	44.0 (7.5)

Note.—NA indicates not applicable; UHDRS, Unified HD Rating Scale. Data are the mean (standard deviation).

* Close participants were significantly older than far participants ($P < .05$).

† Close participants had a significantly longer CAG repeat size than that of far participants ($P < .05$).

‡ In the close group, onset was predicted significantly earlier than in the far group ($P < .001$).

Activation tasks that reliably and selectively activate the striatum in healthy individuals can potentially provide biologic markers for early change in pre-HD. Mounting evidence suggests that the nigrostriatal dopaminergic system underlies our perception and reproduction of temporal information. Pharmacologic manipulation of striatal dopamine neurotransmission disrupts behaviors that involve precise timing in animals (13) and humans (14). In addition, impaired temporal processing has been observed in unmedicated patients with Parkinson's disease (PD), with improvement associated with the initiation of dopamine replacement (15, 16). Results of an fMRI investigation of time discrimination in healthy individuals suggested that the basal ganglia are selectively activated during the encoding of temporal information (17). To our knowledge, no formal studies of temporal processing have been conducted in individuals with pre-HD. Individuals with manifest HD, however, have impaired timing of a conditioned eyeblink response (18).

The present study was performed to investigate functional activation of the basal ganglia in two groups of pre-HD individuals categorized using an estimate of their expected number of years until manifest HD onset based on their CAG repeat length (19). Both groups were compared with a demographically matched control group of healthy individuals. The purpose of this investigation was twofold: 1) to determine if pre-HD patients have a selective performance decrement on a time-discrimination task and 2) to determine if fMRI is sensitive to subtle functional brain changes in pre-HD by using the same task previously shown to activate the basal ganglia in healthy participants (17). We hypothesized that pre-HD participants are less proficient than healthy participants in a time-discrimination task and that this pre-HD performance decrement is associated with a corresponding decrease in task-related activation of the basal ganglia.

Methods

Participants

Participants were 14 individuals who underwent genetic testing that confirmed CAG expansion of the HD gene and seven age- and education-matched control subjects. Participants were excluded if they previously or currently met criteria for manifest HD or if they had a history of other neurologic disturbance (e.g., seizures, head injury), learning disability or mental retardation, major psychiatric disturbance, or substance abuse. All participants were strongly right handed, as determined by scores on the Edinburgh Handedness Inventory (20), and they gave their written informed consent according to guidelines of the Institutional Review Board of the Medical College of Wisconsin, Milwaukee.

Predicted age at motor symptom onset was estimated by using a survival analysis regression equation based on CAG repeat length. Age-conditional expectations of time to onset were derived from this equation. The survival model, co-developed by two of the authors (D.R.L., J.S.P.) expanded on work originally reported by Brinkman et al (21) and was based on 2298 affected and 615 presymptomatic gene-positive HD cases registered at 39 care centers. The analysis was limited to CAG lengths between 41 and 56. Convergent evidence based on nonparametric survival analysis, goodness-of-fit tests, and population genetic models of anticipation in trinucleotide repeat mutations suggested that the participants examined were representative of the entire population with CAG expansion in that range. By using this model, pre-HD participants were assigned to two groups based on estimated proximity to manifest disease onset. Using current ages and CAG expansion lengths, we estimated that seven participants were <12 years from predicted diagnosis of manifest HD; they constituted the close group. Seven participants were estimated to be >12 years from onset; they formed the far group.

Subject demographics are presented in the Table. As expected, compared with those in far group, participants in the close group were significantly older ($P < .05$), they had larger mean CAG repeat length ($P < .05$), and they had earlier estimated years to symptom onset ($P < .001$). The mean age of control subjects did not differ significantly from that of either pre-HD group. The three groups did not differ with respect to years of education.

Before imaging, all pre-HD participants underwent screening for symptoms of manifest HD by using the motor, cognitive, and behavioral scales from the UHDRS (22). Ratings on the UHDRS motor scale (Table) confirmed that gene-positive participants were presymptomatic with low motor-abnormality

scores. Close and far participants did not differ significantly from each other on the UHDRS motor, cognitive, or behavioral scales. Pre-HD participants did not differ significantly from control participants on the cognitive screen of the UHDRS.

Experimental Design

Participants performed three tasks with one imaging run per task (see reference 17 for details). The order of presentation was counterbalanced across participants. In the time-discrimination (T) task, two tones (50 milliseconds) separated by 1200 milliseconds were presented (the standard tone-pair), followed by a 1-second delay and the presentation of a comparison pair of tones. Participants indicated whether the interval defined by the comparison tone-pair was shorter or longer than the first. To better separate neural systems specific to timing operations, participants also performed a pitch-discrimination (P) task in which the auditory events were similar to the T task, except that participants indicated whether the fourth tone was higher or lower in pitch than the first three tones. Imaging runs of each discrimination task were contrasted with a sensorimotor control (C) task in which participants responded after the presentation of two isochronous tone pairs of identical pitch.

Tone stimuli were presented binaurally by using a computer playback system. Sounds were amplified near the scanner and delivered to the participant via air conduction through 180-cm paired plastic tubes, which were threaded through occlusive ear inserts that attenuated background scanner noise to a sound pressure level of approximately 75-dB. Background scanner noise consisted of pulses occurring every 132 milliseconds throughout the imaging run; the intensity of the tone stimuli had an average sound pressure level of 100 dB. For all three tasks, the standard tones were 700 Hz in pitch separated by a 1200-millisecond interval. In the T task, the eight comparison intervals were ±60-millisecond increments of the standard interval. These were presented twice in random order (16 trials); the pitch did not vary across the four tones. In the P task, the eight comparison tone pitches were ±4-Hz increments of the standard 700-Hz tones and presented twice in random order (16 trials); the duration did not vary during this task. In the C task, 16 trials of identical standard tones were presented. Participants pressed one of two keys with their right index or middle finger to indicate shorter/lower or longer/higher in the discrimination tasks. Participants pressed a key by using their right index finger in the C task. Accuracy and reaction time were measured with a nonferrous key-press pad. Participants briefly practiced the three tasks before imaging.

Image Acquisition

Event-related fMRI was performed with a 1.5-T scanner (Signa; GE Medical Systems, Milwaukee, WI) equipped with a three-axis, local-gradient head coil and an elliptical end-capped quadrature radio-frequency coil. Foam padding was used to limit head motion in the coil. Before functional imaging, high-resolution, 3D, spoiled gradient-recalled at steady-state images were collected (TR/TE/NEX = 24/5/1, flip angle = 40°, section thickness = 1.2 mm, field of view = 24 cm, resolution = 256 × 128) for anatomic localization and coregistration. For functional imaging, echo-planar images were collected by using a single-shot, blipped gradient-echo, echo-planar pulse sequence (TR/TE = 2.5/40, flip angle = 90°, field of view = 24 cm, resolution = 64 × 64). Nineteen contiguous, 7-mm-thick sagittal sections were acquired to provide coverage of the entire brain. Imaging was synchronized with the onset of the first tone so that seven images were acquired during each 17.5-second trial. There were 16 trials per run. An additional four images (10.0 seconds) were added to the beginning of the run to allow the MR signal intensity to reach equilibrium, and four images were added to the end of the run to accommodate the delay of the hemodynamic response. Overall, 120 images were collected per run.

fMRI Data Analysis

Functional images were analyzed by using Analysis of Functional NeuroImages (AFNI) software (23). Image time series were spatially registered to reduce the effects of head motion. 3D registration yielded six movement indices per functional imaging run: rotation in the superoinferior, anteroposterior, and left-right planes in degrees, and translation in the superoinferior, anteroposterior, and left-right planes in millimeters. Before movement correction, the root-mean-square difference between the baseline image and all subsequent images in the time series was computed as an index of subject head movement. No significant differences were observed in root-mean-square between the groups, with F(2, 18) = 2.09 and P = .15.

Deconvolution of the fMRI signal intensity was performed on a voxelwise basis. Deconvolution produces time courses that estimate the best-fitting hemodynamic response for each task relative to a baseline resting state. The reference function consisted of impulses at the start of each trial. These impulses were used to deconvolve a model hemodynamic time course without making *a priori* assumptions regarding its shape, delay or magnitude of the impulse response function. The T and P tasks were compared with the C task for the volume collected 7.5 seconds after trial onset (corresponding to the peak of the evoked hemodynamic response). Anatomic and T, P, and C functional images were then interpolated to volumes with 1-mm^3 voxels, coregistered, converted to stereotaxic coordinate space (24), and blurred by using a gaussian filter of 4-mm full-width at half-maximum. Analysis of variance with post-hoc *t* tests by using variance pooled across all participants was performed on a voxelwise basis on the hemodynamic time course estimates at 7.5 seconds after trial onset to identify regions showing greater activation in the T or P tasks than the C task. A *t* value of 3.061 (P < .01, df = 12, uncorrected) was used with a minimum 200-μL (2.04 voxel) cluster threshold to determine statistical significance. A P value of .01 was used because of the small sample.

Regions of Interest

Regions of interest were defined to analyze activation volumes within each isolated region. These regions included the thalamus, caudate, putamen, and presupplementary motor area (pre-SMA)/cingulate and were defined by using the AFNI Talairach daemon (25). The pre-SMA and cingulate regions were defined by using Brodmann areas 6, 24 and 32, but including only those voxels that fell between x = −15 and x = 15 (separating medial from lateral) and from y = 0 (anterior commissure) to y = 30. The SMA was defined by using Brodmann area 6, but including only those voxels posterior to y = 0 and between x = −15 and x = 15. The thalamus, caudate and putamen were defined by using the Talairach daemon. A mask of each region was created and blurred by using a 2-mm full-width at half-maximum gaussian filter. The mask was then applied to the thresholded functional group dataset at 7.5 seconds after trial onset.

Volumetric Analysis

Two raters blinded to group assignment outlined the volumetric measurements of the caudate on the high-resolution anatomic images. Structures were traced in the axial plane by using the Gyrus Finder software plug-in program in AFNI (23). For the caudate head, measurements began 1-mm superior to the axial plane defined by the anterior and posterior commissures. Tracing continued in a superior direction, and stopped 1-mm below the section upon which the confluence of the lateral ventricle first became visible. The medial boundary was defined by the lateral ventricles, and the lateral border of the
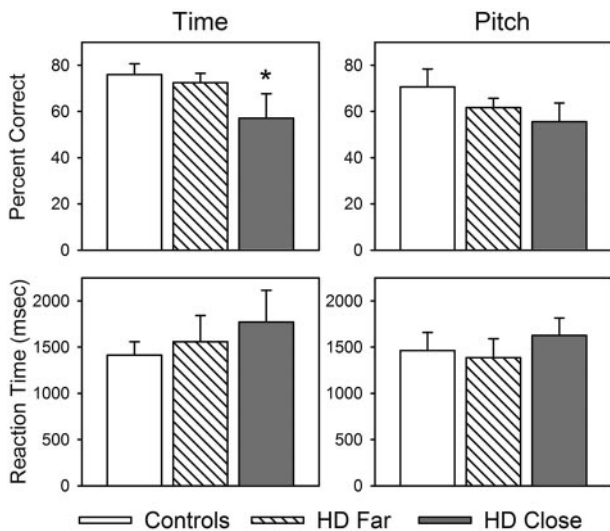
FIG 1.   Mean percentage of correct responses and reaction times for T and P tasks for the control, far, and close groups. *Asterisk* indicates close < control participants (*P* < .05).

caudate was defined by the external capsule. For the caudate body, tracing began at the section where the confluence of the ventricles was first visible and continued in a superior direction until the caudate was no longer visible. The medial border was the lateral ventricle, the superolateral border was the external capsule, and the inferolateral border was the anterior limb of the internal capsule. Interrater reliability was high (r = 0.91).

Results

Task Performance

Figure 1 shows that participants in the close group performed significantly worse than participants in the control group on the T task (t = 1.64, P < .05, one-tailed test), but they performed comparably to control group participants on the P task. No significant group differences in accuracy were observed between far participants and control participants on either the T task or the P task. Likewise, no significant group differences were observed in reaction times for the T or P tasks among the far, close, and control participants.

Structural MR Imaging Measures

Volumetric measurements of the caudate head are presented in Figure 2. Significant group differences in caudate volumes emerged for the left caudate head, with $F(2, 18)$ = 5.41 and P < .05. Post-hoc analysis (Tukey Honestly Significant Difference test) indicated that caudate head volumes were smaller in close participants than in controls. No significant differences were observed for the right caudate head or for the right or left caudate body.

fMRI Activation Data

Figure 3 displays the significant clusters of activation derived from the T-minus-C comparison for the three groups overlaid on anatomic images. The T task

produced unique clusters of activation in the bilateral basal ganglia in control participants, consistent with our previous findings in healthy control participants (17). The center of activation was located in the caudate head and extended laterally into the putamen. The T task also produced foci of activation in the bilateral thalamus and pre-SMA/cingulate. A decrement in the volume of activation was observed in subcortical regions (thalamus, caudate/putamen) as a function of CAG status, with control participants having the largest volume, close participants the smallest, and far participants an intermediate volume. A different pattern emerged in the pre-SMA/cingulate: Far participants had the largest volume of activation, whereas close participants had the smallest volume, and control subjects had an intermediate volume. Total group volumes of the activation clusters for the thalamus, caudate/putamen, and pre-SMA/cingulate are summarized in Figure 4. Significant group differences in functional activation patterns did not emerge for the P-minus-C comparison.

Discussion

The present findings demonstrate that fMRI is sensitive to changes in striatal function long before the emergence of motor symptoms in pre-HD. This observation has several important implications. First, fMRI can potentially be used to identify early neural degeneration before the onset of clinical symptoms. In close participants, subcortical structures were activated significantly less than they were in control participants, whereas far participants had an intermediate level of activation. Neither close participants nor far participants had cognitive or motor deficits in behavior, as measured with the UHDRS, although there were significant differences in performance between control participants and close participants on the T task. Despite changes in neural activation in both groups, structural changes in the caudate were observed only in close participants. This change in neural activation in the close group may be attributed to cell death, since caudate structural atrophy was observed in this group; however, structural atrophy was not observed in far participants, although there was a change in neural activation.

Second, fMRI may be a useful tool for determining the optimal window for treatments aimed at slowing disease progression. Compounds that slow disease progression in animal models are currently undergoing human clinical trials. fMRI may be able to detect the earliest signs of neural degeneration when these treatments are most effective, and fMRI could potentially be used to track the effectiveness of such treatments in slowing neural degeneration.

Third, fMRI may improve the prediction of when HD manifests in an individual. Currently, predictions of manifest HD are based on CAG repeat length or on this length combined with parental age of onset (21). Adding fMRI results to this regression formula may substantially increase the accuracy with which the time of symptom onset is predicted.
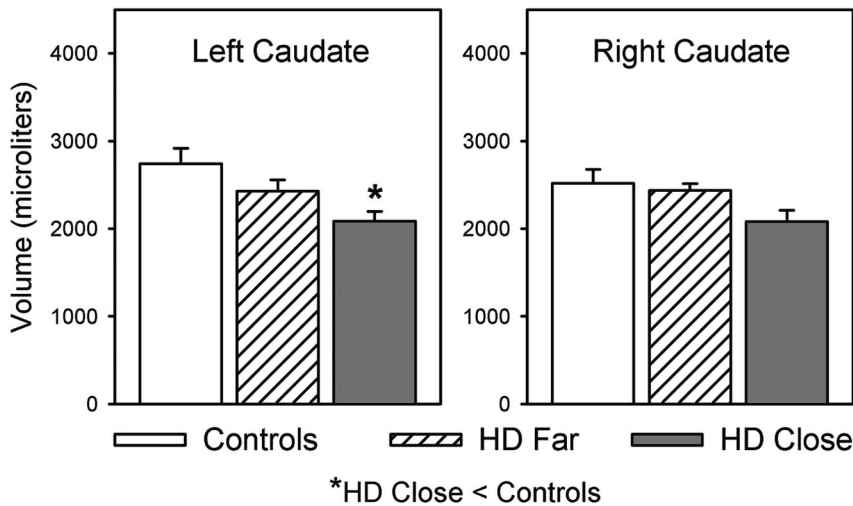
FIG 2.   Mean volumes of the left and right heads of the caudate for the control, far, and close groups. *Asterisk* indicates close < control participants ($P < .05$).
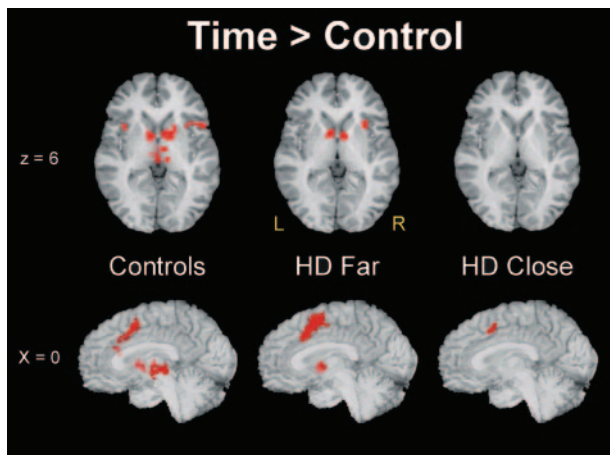

FIG 3.   Activation foci ($P < .01$) derived from the T-minus-C comparison for the control, far, and close groups. *Top row*, Axial sections are 6 mm superior to the anterior commissure–posterior commissure line. *Bottom row*, Sections represent the midsagittal plane.

An interesting finding of the present study is the hyperactivation in medial hemispheric structures (pre-SMA and cingulate) in the far group relative to both the control and close groups. Because behavioral performance of the far group was comparable to that of the control group, this hyperactivation may compensate for reduced subcortical activation in this pre-HD population. Studies of patients with manifest HD and PD support the notion of compensatory increased activation in certain brain areas to maintain normal task performance. For example, positron emission tomographic studies in manifest HD demonstrate different patterns of neural activation relative to control participants during paced movements (26, 27). Most of this activation was reduced relative to control participants; however, increased activation in bilateral insula was suggested to be compensatory (27). Similarly, an fMRI study demonstrated greater activation in lateral premotor regions in individuals with PD during a paced finger-tapping task; the activation partially normalized with dopamine replacement. This lateral premotor hyperactivation in PD was

suggested to compensate for striatal hypofunction during motor tasks (28).

Alternatively, hyperactivation in fMRI may reflect early abnormal cell processes that are direct negative effects of the HD-causing CAG expansion of the gene *Htt* coding for the protein huntingtin (1). Studies of pathogenic mechanisms for HD have eluded cell biologists to date (29). There are no data to address the issue of whether the expanded *Htt* causes dysfunction from within the affected cells in the striatum or from without. Hyperactivation in frontal circuitry seen on fMRI could signal primary HD dysfunction. This speculation is supported by early and progressive electrophysiologic alterations evident in cortical neurons in the R6/2 transgenic mouse model of HD (30). These findings suggest that HD might cause alterations in neuronal function that render glutamatergic corticostriatal projection neurons destructive to the medium spiny neostriatal neurons on which they synapse. However, the mechanisms underlying this process are still unclear. Other electrophysiologic evidence comes from the observation that homovanillic acid Ca^{2+} channels in corticostriatal projection neurons in R6/2 mice have enhanced current attenuation and increased activity (31). Further clarification of the physiologic properties of corticostriatal projection neurons may elucidate the neurodegeneration observed in HD.

Behaviorally, close participants performed more poorly on the T task than control participants. However, far participants performed comparably to control participants. The present results confirm those of several neuropsychological reports suggesting that cognitive performance is impaired long before motor manifestation of HD (32, 33) and worsens as onset approaches (10). On the basis of the current results, we cannot determine how early timing performance is impaired in pre-HD. Longitudinal assessment is important to confirm the onset estimations.

Caudate volume was reduced bilaterally in close participants relative to control participants. These findings are consistent with those of many neuroimaging and neuropathologic studies showing striatal
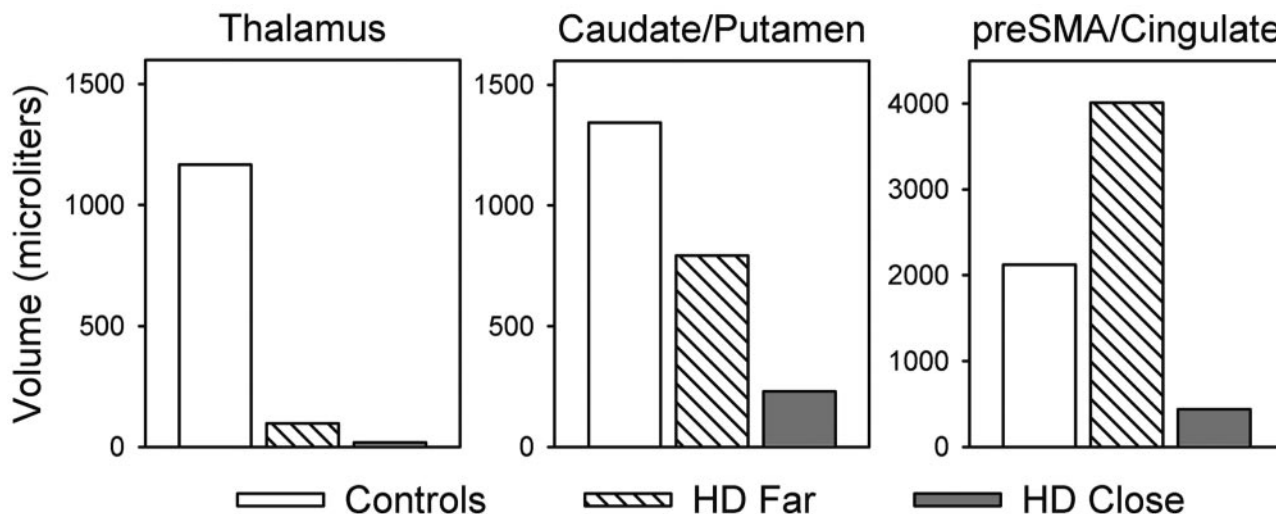
FIG 4.   Volume of activation in the thalamus, caudate/putamen, and pre-SMA/cingulate derived from the time-minus-control subtraction for the control, far, and close groups.

reductions in pre-HD individuals (8, 34–37). Caudate and putaminal volumes have been correlated with symptom severity (38, 39), cognitive performance (40), and estimated years to onset in pre-HD (37). Aylward et al (8, 36, 37) were the first to demonstrate atrophy in a sample of pre-HD individuals. The current findings replicate their results and confirm a relationship between volumetric MR imaging indices and estimated years to disease onset. Although our morphologic findings replicate those of Aylward et al, all MR imaging studies of pre-HD published to date are limited by sample size (e.g., Aylward et al report putaminal volumes for five pre-HD individuals with estimated onset >12 years).

The present study extends previous work supporting the role of the basal ganglia in time perception and reproduction. Although pre-HD individuals in the present study did not demonstrate cognitive or motor deficits on the UHDRS, deficits in temporal processing were identified, consistent with previous studies of individuals with idiopathic PD (15, 16, 41, 42). PD patients, for example, tap at faster rates (16) and exhibit deficits in temporal discrimination relative to control subjects (15, 41, 42). Temporal processing deficits in PD improve with dopamine replacement (15, 16). Close pre-HD individuals were characterized by poor performance on the T task, decreased neural activation of subcortical structures, and volume reductions in the head of the caudate.

The current study was preliminary and could have been strengthened by including a greater number of pre-HD participants. The results of this cross-sectional study demonstrated that fMRI was sensitive to early changes in neural activation in pre-HD populations, even before the advent of behavioral or structural changes. Applying fMRI longitudinally to examine the presymptomatic rate of change in neural structures may provide further insight into the neurodegenerative processes underlying HD.

Conclusion

To our knowledge, our investigation was the first task-activated functional imaging study of a pre-HD sample. This fMRI study demonstrated that pre-HD individuals >12 years from estimated onset of motor symptoms had *decreased* caudate activity and a compensatory *increase* in activity of the supplementary motor area and anterior cingulate during performance of a T task. These differences were not associated with changes in cognitive task performance or brain structure. In contrast, pre-HD patients <12 years from estimated onset of motor symptoms had across-the-board abnormalities in brain activation, task performance, and structural imaging. These cross-sectional results suggest that functional neuroimaging measures may prove useful for tracking the evolution of changes in neural function during the earliest stages of pre-HD.

Acknowledgement

References

1. **The Huntington's Disease Collaborative Research Group: a novel gene containing a trinucleotide repeat that is expanded and unstable on Huntington's disease chromosomes**. *Cell* 1993;72:971–983
2. Vonsattel JP, Myers RH, Stevens TJ, Ferrante RJ, Bird ED, Richardson EP Jr. **Neuropathological classification of Huntington's disease.** *J Neuropathol Exp Neurol* 1985;44:559–577
3. Myers RH, Vonsattel JP, Stevens TJ, et al. **Clinical and neuropathologic assessment of severity in Huntington's disease.** *Neurology* 1988;38:341–347
4. Wagster MV, Hedreen JC, Peyser CE, Folstein SE, Ross CA. **Selective loss of [3H]kainic acid and [3H]AMPA binding in layer VI of frontal cortex in Huntington's disease.** *Exp Neurol* 1994;127:70–75
5. Sotrel A, Paskevich PA, Kiely DK, Bird ED, Williams RS, Myers RH. **Morphometric analysis of the prefrontal cortex in Huntington's disease.** *Neurology* 1991;41:1117–1123

6. Hedreen JC, Peyser CE, Folstein SE, Ross CA. **Neuronal loss in layers V and VI of cerebral cortex in Huntington's disease.** *Neurosci Lett* 1991;133:257–261

7. Campodonico JR, Aylward E, Codori AM, et al. **When does Huntington's disease begin?** *J Intl Neuropsychol Soc* 1998;4:467–473

8. Aylward EH, Codori AM, Rosenblatt A, et al. **Rate of caudate atrophy in presymptomatic and symptomatic stages of Huntington's disease.** *Mov Disord* 2000;15:552–560

9. Harris GJ, Codori AM, Lewis RF, Schmidt E, Bedi A, Brandt J. **Reduced basal ganglia blood flow and volume in pre-symptomatic, gene-tested persons at-risk for Huntington's disease.** *Brain* 1999;122:1667–1678

10. Paulsen JS, Zhao H, Stout JC, et al. **Clinical markers of early disease in persons near onset of Huntington's disease.** *Neurology* 2001;57:658–662

11. Chen M, Ona VO, Li M, et al. **Minocycline inhibits caspase-1 and caspase-3 expression and delays mortality in a transgenic mouse model of Huntington disease.** *Nat Med* 2000;6:797–801

12. Dedeoglu A, Kubilus JK, Yang L, et al. **Creatine therapy provides neuroprotection after onset of clinical symptoms in Huntington's disease transgenic mice.** *J Neurochem* 2003;85:1359–1367

13. Maricq AV, Church RM. **The differential effects of haloperidol and methamphetamine on time estimation in the rat.** *Psychopharmacology (Berl)* 1983;79:10–15

14. Rammsayer TH. **Neuropharmacological evidence for different timing mechanisms in humans.** *Q J Exp Psychol B* 1999;52:273–286

15. Artieda J, Pastor MA, Lacruz F, Obeso JA. **Temporal discrimination is abnormal in Parkinson's disease.** *Brain* 1992;115:199–210

16. O'Boyle DJ, Freeman JS, Cody FW. **The accuracy and precision of timing of self-paced, repetitive movements in subjects with Parkinson's disease.** *Brain* 1996;119:51–70

17. Rao SM, Mayer AR, Harrington DL. **The evolution of brain activation during temporal processing.** *Nat Neurosci* 2001;4:317–323

18. Woodruff-Pak DS, Papka M. **Huntington's disease and eyeblink classical conditioning: normal learning but abnormal timing.** *J Intl Neuropsychol Soc* 1996;2:323–334

19. Langbehn DR, Brinkmann RR, Falush D, Paulsen JS, Hayden MR. **A new model for prediction of age of onset and penetrance for Huntington's Disease based on CAG length.** *Clin Genet* 2004;65:267–277

20. Oldfield RC. **The assessment and analysis of handedness: the Edinburgh Inventory.** *Neuropsychologia* 1971;9:97–113

21. Brinkman RR, Mezei MM, Theilmann J, Almqvist E, Hayden MR. **The likelihood of being affected with Huntington disease by a particular age, for a specific CAG size.** *Am J Hum Genet* 1997;60:1202–1210

22. Huntington Study Group. **Unified Huntington's Disease Rating Scale: reliability and consistency.** *Mov Disord* 1996;11:136–142

23. Cox RW. **AFNI: software for analysis and visualization of functional magnetic resonance neuroimages.** *Comput Biomed Res* 1996;29:162–173

24. Talairach J, Tournoux P. *Co-planar Stereotaxic Atlas of the Human Brain.* New York: Thieme, 1988

25. Lancaster JL, Woldorff MG, Parsons LM, et al. **Automated Talairach atlas labels for functional brain mapping.** *Hum Brain Mapp* 2000;10:120–131

26. Weeks RA, Ceballos-Baumann A, Piccini P, Boecker H, Harding AE, Brooks DJ. **Cortical control of movement in Huntington's disease: a PET activation study.** *Brain* 1997;120:1569–1578

27. Bartenstein P, Weindl A, Spiegel S, et al. **Central motor processing in Huntington's disease: a PET study.** *Brain* 1997;120:1553–1567

28. Haslinger B, Erhard P, Kampfe N, et al. **Event-related functional magnetic resonance imaging in Parkinson's disease before and after levodopa.** *Brain* 2001;124:558–570

29. Tobin AJ, Signer ER. **Huntington's disease: the challenge for cell biologists.** *Trends Cell Biol* 2000;10:531–536

30. Cepeda C, Ariano MA, Calvert CR, et al. **NMDA receptor function in mouse models of Huntington disease.** *J Neurosci Res* 2001;66:525–539

31. Cherry JA, Thompson BE, Pho V. **Diazepam and rolipram differentially inhibit cyclic AMP-specific phosphodiesterases PDE4A1 and PDE4B3 in the mouse.** *Biochim Biophys Acta* 2001;1518:27–35

32. Foroud T, Siemers E, Kleindorfer D, et al. **Cognitive scores in carriers of Huntington's disease gene compared to noncarriers.** *Ann Neurol* 1995;37:657–664

33. Lawrence AD, Hodges JR, Rosser AE, et al. **Evidence for specific cognitive deficits in preclinical Huntington's disease.** *Brain* 1998;121:1329–1341

34. Albin RL, Reiner A, Anderson KD, et al. **Preferential loss of striato-external pallidal projection neurons in presymptomatic Huntington's disease.** *Ann Neurol* 1992;31:425–430

35. Albin RL, Young AB, Penney JB, et al. **Abnormalities of striatal projection neurons and N-methyl-D-aspartate receptors in presymptomatic Huntington's disease.** *N Engl J Med* 1990;322:1293–1298

36. Aylward EH, Brandt J, Codori AM, Mangus RS, Barta PE, Harris GJ. **Reduced basal ganglia volume associated with the gene for Huntington's disease in asymptomatic at-risk persons.** *Neurology* 1994;44:823–828

37. Aylward EH, Codori AM, Barta PE, Pearlson GD, Harris GJ, Brandt J. **Basal ganglia volume and proximity to onset in presymptomatic Huntington disease.** *Arch Neurol* 1996;53:1293–1296

38. Harris GJ, Pearlson GD, Peyser CE, et al. **Putamen volume reduction on magnetic resonance imaging exceeds caudate changes in mild Huntington's disease.** *Ann Neurol* 1992;31:69–75

39. Starkstein SE, Brandt J, Bylsma F, Peyser C, Folstein M, Folstein SE. **Neuropsychological correlates of brain atrophy in Huntington's disease: a magnetic resonance imaging study.** *Neuroradiology* 1992;34:487–489

40. Campodonico JR, Codori AM, Brandt J. **Neuropsychological stability over two years in asymptomatic carriers of the Huntington's disease mutation.** *J Neurol Neurosurg Psychiatry* 1996;61:621–624

41. Riesen JM, Schnider A. **Time estimation in Parkinson's disease: normal long duration estimation despite impaired short duration discrimination.** *J Neurol* 2001;248:27–35

42. Harrington DL, Haaland KY, Hermanowicz N. **Temporal processing in the basal ganglia.** *Neuropsychology* 1998;12:3–12